Acta Cryst. (1995). D51, 529–535

Structure-Based Design of Inhibitors of Purine Nucleoside Phosphorylase

BY Y. SUDHAKAR BABU*

BioCryst Pharmaceuticals, Inc., 2190 *Parkway Lake Drive, Birmingham, AL* 35244, *USA*

STEVEN E. EALICK†

Center for Macromolecular Crystallography, University of Alabama at Birmingham, University Station, Birmingham, AL 35294-2010, *USA*

CHARLES E. BUGG

BioCryst Pharmaceuticals, Inc., 2190 *Parkway Lake Drive, Birmingham, AL* 35244, *USA*

MARK D. ERION‡ AND WAYNE C. GUIDA

CIBA-GEIGY Corporation, 556 *Morris Avenue, Summit, NJ* 07901, *USA*

JOHN A. MONTGOMERY

BioCryst Pharmaceuticals, Inc., 2190 *Parkway Lake Drive, Birmingham, AL* 35244, *USA*

AND JOHN A. SECRIST III

Southern Research Institute, PO Box 55305, *Birmingham, AL* 35255-5305, *USA*

(*Received* 25 *July* 1994; *accepted* 14 *October* 1994)

Abstract

Inhibitors of purine nucleoside phosphorylase may have therapeutic value in the treatment of T-cell proliferative diseases such as T-cell leukemia, in the suppression of host-*versus*-graft response in organ transplants, and in the treatment of T-cell-mediated autoimmune diseases. Competitive inhibitors of this enzyme have been designed using the three-dimensional structure of the enzyme determined by X-ray crystallography. This approach has resulted in the synthesis of the most potent and membrane-permeable inhibitors of purine nucleoside phosphorylase reported so far.

Introduction

The search for new chemical entities is the cornerstone of the drug discovery process. Most drugs that are in use today were discovered more or less empirically. The two prevailing methods of drug discovery are the 'screening method' and 'rational' drug design. Most pharmaceutical companies today employ some form of rational drug-design methodology although screening is also routinely practiced. Besides being random, screening is inherently repetitious and time consuming. Even lead optimization by means of structural modifications to an active compound is primarily a trial-and-error process, even though the probability of success is much greater than a purely random process. A number of different approaches have been developed to make this approach more efficient.

Recent advances in biotechnology, macromolecular crystallography, computer graphics and related fields have led to a new approach in drug discovery called structure-based drug design. Structure-based drug design is the discovery of drugs based on a detailed structural knowledge of the target (enzyme or receptor) and the interaction of small molecules with it. Clearly, structural information in combination with graphical methods for displaying accessible volume, electrostatic potential and hydrophobicity of the active site of the target macromolecule greatly facilitates the drug-design process. Further enhancement in the quality of the 'designed compounds' is expected from methods that can accurately evaluate the target molecule in terms of binding conformation, binding affinity and binding-induced conformational changes in the protein. Accurate prediction of binding affinities and protein conformational changes are currently not routinely possible although significant advances are being made.

* To whom correspondence should be addressed.

† Present address: Department of Biochemistry, Cornell University, 207 Biotechnology Building, Ithaca, NY 14853, USA.

‡ Present address: Gensia Pharmaceuticals, Inc., 4575 Eastgate Mall, San Diego, CA 92121, USA.

The foundation of structure-based drug design is the detailed information about the three-dimensional molecular structure of the target macromolecule *e.g.* enzymes and receptors. Fig. 1 outlines the overall strategy of this approach. At the present time, X-ray crystallography is the preferred technique for obtaining the atomic resolution structural data that would usually be required for drug design. Recently, we at BioCryst have successfully completed a project to design and synthesize potent inhibitors of the enzyme purine nucleoside phosphorylase (PNP) using the three-dimensional structure of the active site of the enzyme (Ealick *et al.*, 1991). The application of structured-based drug design in this project is the subject of this article.

Purine nucleoside phosphorylase (PNP, E.C. 2.4.2.1) catalyzes the reversible phosphorylysis of ribonucleosides and 2′-deoxyribonucleosides of guanine, hypoxanthine and a number of related nucleoside analogs (Parks & Agarwal, 1972). Although under equilibrium conditions the isolated enzyme catalyzes the nucleoside synthesis, it normally acts in the phosphorolytic direction in intact cells.

Interest in PNP as a drug target arises from its ability to rapidly metabolize purine nucleosides and from its role in the T-cell branch of the immune system. The high level of PNP activity *in vivo* suggests that the chemotherapeutic potential of certain purine nucleoside analogs may be severely compromised by PNP metabolism. These include the potential anticancer agent 2′-deoxy-6-thioguanosine (LePage, Junga & Bowman, 1964), and the anti-AIDS drug 2′,3′-dideoxyinosine (Erion, 1990). Hence, a combination of a PNP inhibitor and these purine-nucleoside analogs may prove to be more efficacious. PNP inhibitors by themselves have potential therapeutic value based on the finding that patients lacking PNP activity exhibit severe T-cell immunodeficiency while maintaining normal or exaggerated B-cell function. This profile suggests that PNP inhibitors might be useful in the treatment of T-cell proliferative diseases such as T-cell leukemia or T-cell lymphoma, in the suppression of the host-*versus*-graft response in organ transplant patients, and in the treatment of T-cell mediated autoimmune diseases such as rheumatoid arthritis and lupus erythematosus (Otterness & Bilven, 1989). Despite the potential benefits of PNP inhibitors and despite the large number of PNP inhibitors

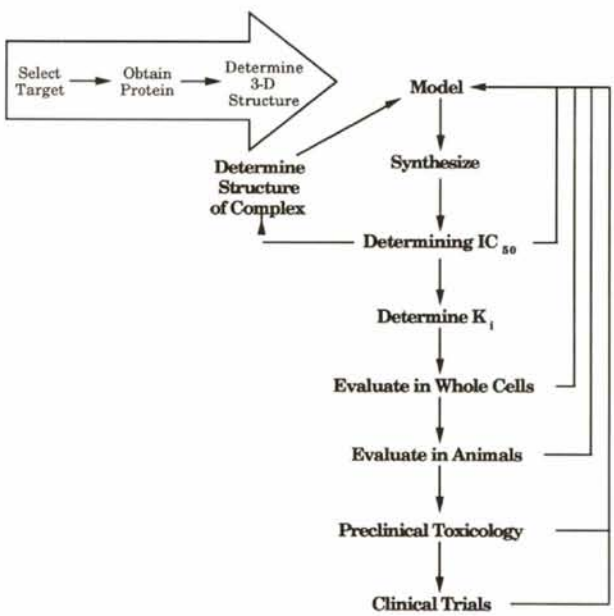

Fig. 1. Flow chart showing the strategy for structure-based drug design.

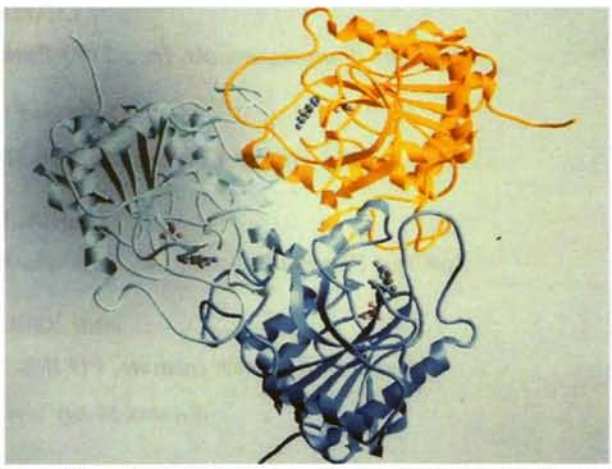

Fig. 2. Three-dimensional structure of human PNP trimer. Guanine and phosphate are shown in the active site as ball-and-stick models.

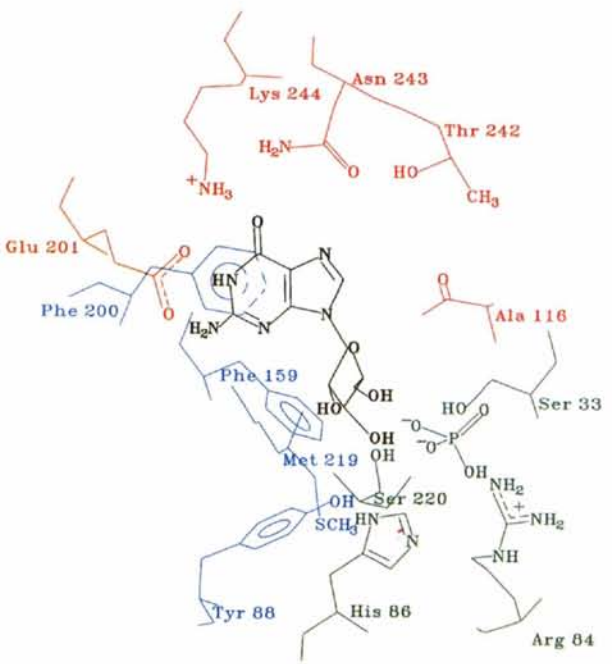

Fig. 3. Binding of guanosine (shown in black) in the active site of PNP. The amino-acid residues that interact with guanine moiety are shown in red, hydrophobic pocket in blue and the phosphate-binding site is shown in green.

that have been synthesized to date, no compound has yet reached clinical trials. One problem is the potency of the membrane-permeable compounds thus far prepared. Although potencies for the best compounds have affinities 10–100 higher than the natural substrate ($K_m \simeq 4\,mM$), it is expected that T-cell immunotoxicity will only occur with very tight binding inhibitors (K_i, $< 10\,nM$) due to the high *in vivo* PNP activity and competition with substrate. Hence, we determined the structure of human PNP by X-ray crystallography and have utilized these results in combination with computer-assisted molecular modeling to design novel highly potent inhibitors of this key enzyme.

Experimental

PNP has been isolated from both eukaryotic and prokaryotic cells (Stoeckler, 1984) and functions in the purine salvage pathway. Human PNP is a trimer of identical subunits with a total molecular weight of about 97 000 Da. Each subunit contains 289 amino-acid residues. Crystals of human PNP for X-ray diffraction studies were grown from ammonium sulfate solution as described previously (Cook, Ealick, Bugg, Stoeckler & Parks, 1981). These crystals are stored in artificial mother liquor solution made up of 60% ammonium sulfate, 0.05 *M* citrate buffer at pH 5.4. The space group is *R*32 with hexagonal cell parameters $a = 142.9\,(1)$ and $c = 165.2\,(1)$ Å. PNP crystals contain about 76% solvent and diffracts to around 2.8 Å resolution. The three-dimensional structure was determined by multiple isomorphous replacement techniques using synchrotron radiation (Ealick *et al.*, 1990). The native and guanine–PNP complex structures have been refined to 2.8 Å resolution.

Structure description

The X-ray analysis confirmed the trimeric nature of the enzyme in which the subunits are related by the crystallographic threefold axis (Fig. 2). Each subunit contains an eight-stranded β-sheet and a five-stranded β-sheet which join to form a distorted β-barrel. Seven α-helices surround this β-sheet structure. The active site is located near the subunit–subunit boundary within the trimer, and involves seven polypeptide segments from one subunit and a short segment from the adjacent subunit. The purine-binding site is composed of residues Glu201, Lys244 and Asn243 which form hydrogen bonds with N1, O6 and N7 of purine (Fig. 3). The remainder of the purine-binding pocket is largely hydrophobic, being composed of residues Ala116, Phe200 and Val217. The phosphate-binding site is composed of residues Ser33, Arg84, His86 and Ser220 with the phosphate positioned for nucleophilic attack at C1 of the nucleoside. The sugar-binding site is mostly hydrophobic consisting of residues Tyr88, Phe159 (of the adjacent subunit), Phe200 and His257. This hydrophobic pocket serves to orient the sugar to facilitate nucleophilic attack by phosphate and subsequent inversion at C1′.

A 'swinging gate' consisting of residues 241–260 controls access to the active site (Fig. 4). This gate,

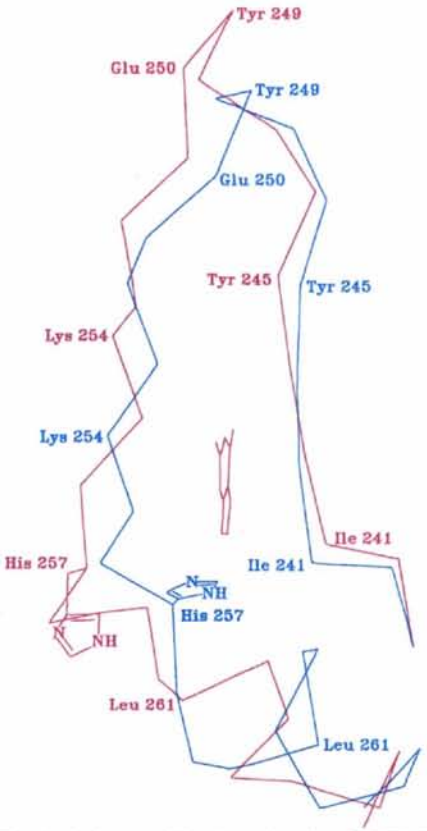

Fig. 4. The 'swinging gate' in the active site of PNP. The guanine–enzyme complex is shown in magenta and the native enzyme in cyan.

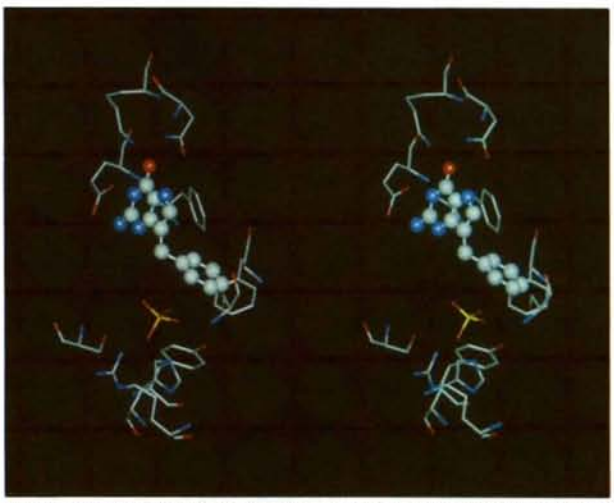

Fig. 5. Binding of 9-benzyl-9-deazaguanine in the active site of PNP. The atoms are shown in different colors, red for O, blue for N, yellow for P and the rest are C atoms.

closed in the native enzyme, opens during substrate binding to accommodate the substrate or a substrate-like competitive inhibitor. The electron density for these residues in the native structure was poorly defined indicating high thermal motion for these residues. The maximum movement caused by substrate or inhibitor binding occurs at His257, which is displaced outwards by several ångströms. The gate is anchored near the central β-sheet at one end and near the C-terminal helix at the other end. The gate movement is complex and appears to involve a helical transformation near residues 257–261. Consequently, initial inhibitor-modeling attempts using the native PNP structure were far less successful than subsequent analyses in which coordinates for the guanine–PNP complex were used. Because of the magnitude of the changes that occur during substrate binding, it is unlikely that modeling studies based on the native structure alone would have accurately predicted the structure of the complex between PNP and purine analog inhibitors.

Structure-based drug design

At the beginning of our studies several PNP inhibitors had been reported with K_i values in the 10^{-6} to 10^{-7} range including 8-aminoguanine (Stoeckler, Cambor, Kuhns, Chu & Parks, 1982), 9-benzyl-8-aminoguanine (Shewach, Chen, Pillote, Townsend & Daddona, 1986), and 5′-iodo-9-deazainosine (Stoeckler *et al.*, 1986). Acyclovir diphosphate had been shown to have a K_i near 10^{-8} if assayed at 1 m*M* phosphate rather than the more frequently used value of 50 m*M* (Tuttle & Krenitsky, 1984). During our studies, the synthesis of 8-amino-9-(2-thienylmethyl)guanine was reported with a K_i of 6.7×10^{-8} *M* (Gilbertsen *et al.*, 1987). In order to understand the interaction of these inhibitors with the active-site residues, these compounds were obtained and crystallographic analyses were carried out. The most important findings were the following: (1) 8-amino substituents enhance binding by forming hydrogen bonds with Thr242 and possibly the carbonyl O atom of Ala116; (2) 9-deaza analogs acquire potency through formation of a hydrogen bond with Asn243; (3) substitution by hydrophobic groups at the 9-position of a purine enhances binding through interaction with hydrophobic region in the ribose-binding site; (4) acyclovir diphosphate is a multisubstrate inhibitor in which the acyclic spacer between N(9) of the purine and the phosphate is near optimal length to accommodate the two binding sites. Based on these results, a number of starting compounds were proposed that incorporated these and other features predicted to enhance inhibitor binding.

9-substituted 9-deaza purine analogs were selected as the first series of PNP inhibitors for synthesis. The first 9-deazaguanine derivatives synthesized, such as 9-benzyl-9-deazaguanine, were three to six times more potent than the most potent known inhibitor, 8-amino-9-(2-thienylmethyl)guanine. Crystallographic data showed (Fig. 5) that the phenyl ring of the 9-benzyl compound tended to optimize its interactions with Phe159 and Phe200, resulting in the classic 'herringbone' arrangement reported in a variety of aromatic systems (Burley & Petsko, 1985). In some cases, ring substitution resulted in displacement of the molecule centroid; however, the ring tilt relative to Phe159 and Phe200 remained relatively constant. The optimum spacer between the purine base and the aromatic substituent appears to be a single methylene group.

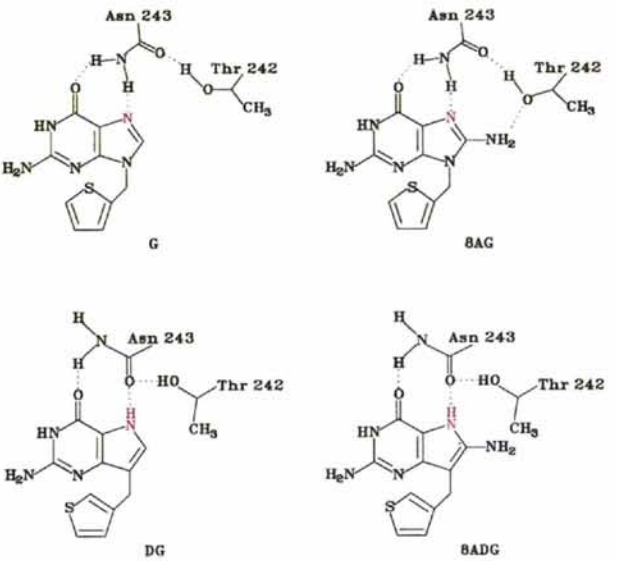

Fig. 6. Crystallographic analysis of four PNP complexes to highlight the effects of 8-amino and 9-deaza modifications. The 9-thienyl substituent is attached to guanine (G), 8-aminoguanine (8AG), 9-deazaguanine (DG) and 8-amino-9-deazaguanine (8ADG). Proposed hydrogen bonds, shown as dotted lines, are derived from the analysis of difference Fourier maps.

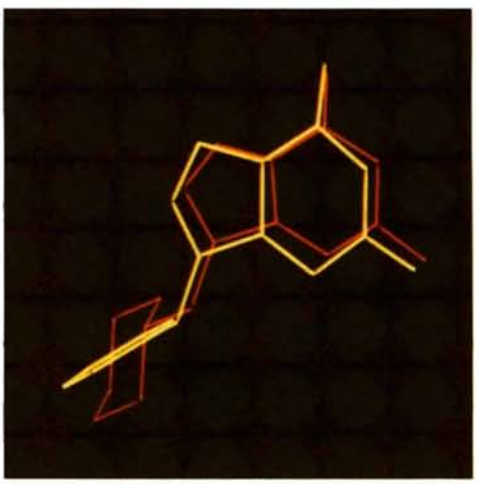

Fig. 7. Comparison of the binding of 9-cyclohexylmethyl-9-deazaguanine with that of 9-benzyl-9-deazaguanine. The cyclohexyl ring occupies the same general space in the active site as the phenyl ring of the benzyl compound.

Table 1. *Effects of* 8-*amino substitution*

Calf spleen PNP was assayed in 50 m*M* phosphate buffer. G, guanine; 8AG, 8-aminoguanine; DG, 9-deazaguanine; 8ADG, 8-amino-9-deazaguanine.

	IC_{50} (μM)			
9-Substituent	G	8AG	DG	8ADG
2-Thienylmethyl	11*	0.16*	0.14	—
3-Thienylmethyl	—	0.085*	0.08	8.0
Benzyl	—	0.47*	0.23	7.7
Cyclohexylmethyl	—	—	2.2	150
3-Methyl-2-thienyl methyl	48*	4*	—	—
2-Furanylmethyl	18*	0.25*	0.31	—

* Human erythrocytic PNP assayed in 50 m*M* phosphate buffer.

Both 8-aminoguanine analogs and 9-deazaguanine analogs are good inhibitors of PNP. However, introduction of an 8-amino group into the 9-deazaguanine derivatives resulted in decreased potency (Table 1). To understand this poor binding, we undertook crystallographic analysis of PNP complexes with four compounds having the 9-thienyl substituent attached to guanine (G), 8-aminoguanine (8AG), 9-deazaguanine (DG) and 8-amino-9-deazaguanine (8ADG). The results of this analysis are summarized in Fig. 6. These data show one mode of binding for compounds that accept a hydrogen bond from Asn243 at N7 (G and 8AG) and another for compounds that donate hydrogen from N7 to Asn243 (DG and 8ADG). The 8-aminoguanine analogs (8AG) make use of the Thr242 side chain to form an additional hydrogen bond which causes an improvement in binding affinity. In the 9-deazaguanine series, where N7 has an attached H atom, Asn243 undergoes a shift that is seen in difference Fourier maps. This shift is probably caused by the formation of the N(7)—H···O(243) hydrogen bond. At the same time, a concomitant shift by Thr242 prevents it from hydrogen bonding to the 8-amino group of the 9-deazaguanine (8ADG). Furthermore, the overall conformational change causes the methyl group of Thr242 to move towards the 8-amino group, thereby generating a hydrophobic environment for the 8-amino group and causing a decrease in binding affinity. This observation, confirmed with other 9-deazaguanine analogs, led us to focus on changes that would have more favourable interactions with the other two subsites.

Inhibitors with cycloaliphatic substituents at N9 of deazaguanine were also as potent as the aromatic analogs. The cycloaliphatic substituents occupied the same general volume as the aromatic groups (Fig. 7). As with the aromatic series, the optimum spacer between the 9-deazaguanine and the hydrophobic substituent is one C atom. X-ray analysis of the PNP complexes of 9-cyclohexyl-9-deazaguanine, a relatively poor inhibitor, and the complex of 9-cyclohexylmethyl-9-deazaguanine showed the surprising result that the two cyclohexyl groups occupy approximately the same general space in the active site and the 9-deazapurine is pulled out of its optimal position in the purine-binding pocket (Fig. 8).

To take full advantage of the binding properties of the PNP active site, it is necessary to design compounds that interact optimally not only with the purine and hydrophobic binding sites but also with the phosphate-binding site (either directly or *via* electrostatic interactions). Starting with a model of the 9-benzyl-9-deazaguanine-PNP complex, we concluded that two of the positions on the 9-benzyl group, namely the 2-position of the phenyl ring and one of the benzylic sites, appeared to be oriented so that a group attached to either one of these positions could interact favourably with the phosphate-binding site. The first compound that was made in this series, 9-[2-(3-phosphonopropoxy)-

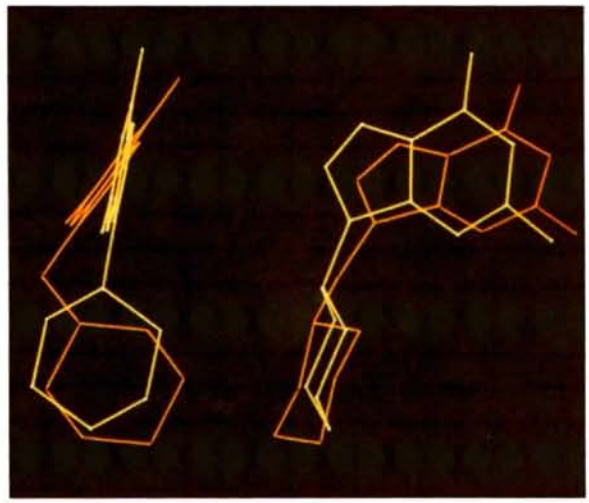

Fig. 8. End view (left) and side view (right) comparison of the binding of 9-cyclohexyl-9-deazaguanine with that of 9-cyclohexylmethyl-9-deazaguanine. The two cyclohexyl groups occupy approximately the same space in the active site, pulling the 9-deazaguanine moiety out of its optimal binding position in the purine-binding site.

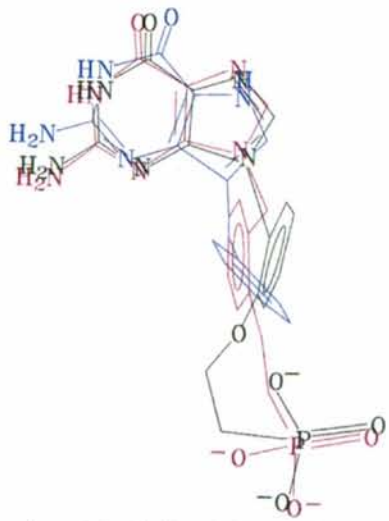

Fig. 9. Comparison of the binding of 9-benzyl-9-deazaguanine (blue) with that of 9-[2-(3-phosphonopropoxy)benzyl]guanine (green) and 9-[2-(1-phosphonoethyl)benzyl]guanine (red).

benzyl]guanine, turned out to be a poor PNP inhibitor. Subsequent crystallographic analysis revealed that the plane of the aromatic ring has rotated approximately 90° from its optimum position in the hydrophobic pocket (Fig. 9). This reorientation of the ring is presumably necessary to accommodate the long spacer (four-atom

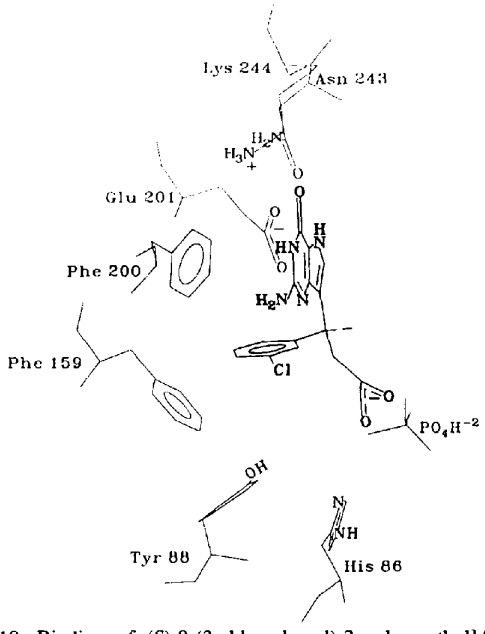

Fig. 10. Binding of (*S*)-9-(3-chlorophenyl)-2-carboxyethyl]-9-deazaguanine in the active site of PNP. The compound is shown in black.

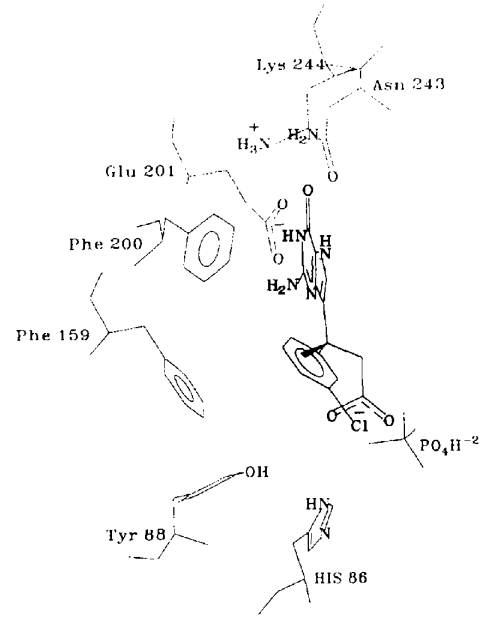

Fig. 11. Binding of (*R*)-9-(3-chlorophenyl)-2-carboxyethyl]-9-deazaguanine in the active site of PNP. The compound is shown in black.

Table 2. *Inhibition data for selected PNP inhibitors by increasing IC_{50} value*

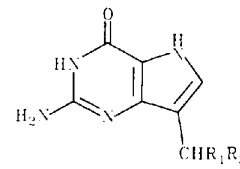

		IC_{50} (μ*M*)		
		50 m*M*	1 m*M*	
R_1*	R_2	phosphate†	phosphate‡	Ratio§
(*S*)-3-Chlorophenyl	CH_2CO_2H	0.031	0.0059	5.3
3-Chlorophenyl	CH_2CN	1.8	0.010	180
2-Tetrahydrothienyl	H	0.22	0.011	20
3,4-Dichlorophenyl	H	0.25	0.012	21
3-Thienyl	H	0.08	0.020	4.0
3-Trifluoromethylcyclohexyl	H	0.74	0.020	37
Cyclopentyl	H	1.8	0.029	62
Cycloheptyl	H	0.86	0.030	29
Pyridin-3-yl	H	0.20	0.030	7.3
2-(Phosphonoethyl)phenyl¶	H	0.45	0.035	13
Cyclohexyl	H	2.0	0.043	47
2-Furanyl	H	0.31	0.085	3.6
(*R*)-3-Chlorophenyl	CH_2CO_2H	0.90	0.16	5.6
2-Phosphonopropoxyphenyl¶	H	42	1.0	42

* Compounds with R_2 not equal to H are racemic mixtures unless the *R* or *S* isomer is designated.
† Calf spleen PNP assayed in 50 m*M* phosphate buffer.
‡ Calf spleen PNP assayed in 1 m*M* phosphate buffer.
§ IC_{50} at 50 m*M* phosphate divided by IC_{50} at 1 m*M* phosphate.
¶ Guanine base.

length) between the phenyl ring and the phosphonate group. A compound with a two-carbon spacer was a much better PNP inhibitor; however, it was clear from X-ray analysis that the aromatic ring was still not able to form an ideal 'herringbone' packing interaction.

Alternatively, compounds were modeled in which the spacer to the phosphate-binding site branched from the benzylic C atom, thus placing no restrictions on the tilt of the aromatic ring. Modeling studies of the 9-benzyl-9-deazaguanine–PNP complex indicated that of the two benzylic positions, one (*pro-R*) pointed into a sterically crowded area within the active site, whereas the other (*pro-S*) pointed into a relatively empty space adjacent to the phosphate-binding site. This analysis led to the synthesis of racemic 9-[1-(3-chlorophenyl)-2-cyanoethyl]-9-deazaguanine and related compounds. The most potent compound of this series was 9-[1-(3-chlorophenyl)-2-carboxyethyl]-9-deazaguanine. This compound was resolved into its (*S*) and (*R*) isomers. As predicted, the (*S*)-acid was 30-fold more potent inhibitor of PNP than the (*R*) isomer and is the most potent membrane-permeable PNP inhibitor reported to date. X-ray crystallographic analysis of the complexes revealed that the (*S*)-acid was oriented properly for optimal interactions with all the three subsites (Fig. 10), whereas the (*R*)-acid was not (Fig. 11).

Crystallographic analysis of a number of inhibitor–PNP complexes revealed variations in the binding of the

inhibitors in the enzyme active site. These differences appear to be the result of close contacts between the inhibitor and the ion in the phosphate-binding site. A sulfate ion occupies the phosphate site in PNP crystals as they are grown from ammonium sulfate solution. These inhibitors were more potent when the binding was measured in 1 m*M* phosphate solution than in 50 m*M* phosphate (Table 2). Kinetic studies showed that these inhibitors are competitive not only with inosine but also with phosphate which is in keeping with the above observation.

This structure-based inhibitor design approach led to a number of inhibitors, which were more than 100 times more potent than any membrane-permeable inhibitor available at the start of this project. During the two and half years of this project, about 60 active compounds were synthesized. This is a remarkably small number compared with the extensive synthesis programmes that are generally involved in drug discovery by trial-and-error techniques. The large number of active compounds and the enhancement of inhibitor potency stand as proof that crystallographic and modeling techniques are now capable of playing a critical role in the rapid discovery of novel therapeutic agents.

We wish to thank Dr W. J. Cook for providing crystals of human PNP.

References

BURLEY, S. K. & PETSKO, G. A. (1985). *Science*, **229**, 23–28.

COOK, W. J., EALICK, S. E., BUGG, C. E., STOECKLER, J. D. & PARKS, R. E. JR (1981). *J. Biol. Chem.* **256**, 4079–4080.

EALICK, S. E., BABU, Y. S., BUGG, C. E., ERION, M. D., GUIDA, W. C., MONTGOMERY, J. A. & SECRIST, J. A. (1991). *Proc. Natl Acad. Sci. USA*, **88**, 11540–11544.

EALICK, S. E., RULE, S. A., CARTER, D. C., GREENHOUGH, T. J., BABU, Y. S., COOK, W. J., HABASH, J., HELLIWELL, J. R., STOECKLER, J. D., PARKS, R. E. JR, CHEN, S.-F. & BUGG, C. E. (1990). *J. Biol. Chem.* **265**, 1812–1820.

ERION, M. D. (1990). Eur. Patent Appl. 374 096.

GILBERTSEN, R. B., SCOTT, M. E., DONG, M. K., KOSSAREK, L. M., BENNETT, M. K., SCHRIER, D. J. & SIRCAR, J. C. (1987). *Agents Actions*, **21**, 272–274.

LEPAGE, G. A., JUNGA, I. G. & BOWMAN, B. (1964). *Cancer Res.* **24**, 835–840.

OTTERNESS, I. & BILVEN, M. (1989). *New Developments in Antirheumatic Therapy* in *Inflammation and Drug Therapy Series*, Vol. 2, edited by K. RAINSFORD & G. VELO, pp. 277–304. Norwell, MA: Kluwer Academic Press.

PARKS, R. E. JR & AGARWAL, R. P. (1972). *The Enzymes*, Vol. 7, edited by P. D. BOYER, pp. 483–514. New York: Academic Press.

SHEWACH, D. S., CHEN, J.-W., PILLOTTE, K. E., TOWNSEND, L. B. & DADDONA, P. E. (1986). *Cancer Res.* **46**, 519–523.

STOECKLER, J. D. (1984). *Developments in Cancer Chemotherapy*, edited by R. E. GLAZER, pp. 35–60. Boca Raton: CRC Press.

STOECKLER, J. D., CAMBOR, C., KUHNS, V., CHU, S.-H. & PARKS, R. E. JR (1982). *Biochem. Pharmacol.* **31**, 163–171.

STOECKLER, J. D., RYDER, J. B., PARKS, R. E. JR, CHU, M.-Y., LIM, M.-I., RAN, W.-Y. & KLEIN, R. S. (1986). *Cancer Res.* **46**, 1774–1778.

TUTTLE, J. V. & KRENITSKY, T. A. (1984). *J. Biol. Chem.* **259**, 4065–4069.